the plant journal

SEB SOCIETY FOR EXPERIMENTAL BIOLOGY

The Plant Journal (2009) **59**, 303–315 doi: 10.1111/j.1365-313X.2009.03870.x

Mutation of the rice gene *PAIR3* results in lack of bivalent formation in meiosis

Wenya Yuan[1], Xingwang Li[1], Yuxiao Chang[1], Ruoyu Wen[2], Guoxing Chen[1], Qifa Zhang[1] and Changyin Wu[1,*]

[1]*National Key Laboratory of Crop Genetic Improvement and National Center of Plant Gene Research (Wuhan), Huazhong Agricultural University, Wuhan 430070, China, and*

[2]*Department of Cell and Developmental Biology, John Innes Centre, Norwich NR4 7UH, UK*

Received 26 November 2008; revised 28 February 2009; accepted 9 March 2009; published online 9 April 2009.

*For correspondence (fax +86 27 87287092; e-mail cywu@mail.hzau.edu.cn).

SUMMARY

Meiosis is essential for eukaryotic sexual reproduction and important for genetic diversity among individuals. Although a number of genes regulating homologous chromosome pairing and synapsis have been identified in the plant kingdom, their molecular basis remains poorly understood. In this study, we identified a novel gene, *PAIR3* (*HOMOLOGOUS PAIRING ABERRATION IN RICE MEIOSIS 3*), required for homologous chromosome pairing and synapsis in rice. Two independent alleles, designated *pair3-1* and *pair3-2*, were identified in our T-DNA insertional mutant library which could not form bivalents due to failure of homologous chromosome pairing and synapsis at diakinesis, resulting in sterility in both male and female gametes. Suppression of *PAIR3* by RNAi produced similar results to the T-DNA insertion lines. *PAIR3* encodes a protein that contains putative coiled-coil motifs, but does not have any close homologs in other organisms. *PAIR3* is preferentially expressed in reproductive organs, especially in pollen mother cells and the ovule tissues during meiosis. Our results suggest that *PAIR3* plays a crucial role in homologous chromosome pairing and synapsis in meiosis.

Keywords: PAIR3, homologous chromosome pairing, meiosis, anther development, embryo sac development.

INTRODUCTION

Meiosis is a highly conserved process in eukaryotes and occupies a central role in the life cycles of all sexually reproducing organisms. It serves to increase the genetic diversity of populations through recombination. In meiosis, a single round of DNA replication is followed by two successive rounds of chromosome segregation (meiosis I and meiosis II), which are necessary for the conversion of diploid cells into the haploid gametes needed for fertilization. Meiosis I is a reductional division involving the segregation of homologous chromosomes, and meiosis II is an equational division involving the segregation of sister chromatids (Ma, 2005). Both meiosis I and meiosis II comprise prophase, metaphase, anaphase and telophase, and prophase I is further divided into five substages, leptotene, zygotene, pachytene, diplotene and diakinesis, characterized by the cytology of the chromosomes (Zickler and Kleckner, 1999).

Prophase I is a long and highly organized process involving sister chromatid cohesion (SCC), homologous chromosome alignment, pairing, synapsis and recombination (Hamant *et al.*, 2006). Sister chromatid cohesion is a multiprotein cohesion complex which is formed initially at the centromere region and then spreads through the whole chromosome to link the sister chromatids together (Hamant *et al.*, 2006). Mutations of the SCC genes, especially the yeast *REC8* homologs such as Arabidopsis *SYN1*/*DIF1* (Bai *et al.*, 1999; Bhatt *et al.*, 1999; Cai *et al.*, 2003), maize (*Zea mays*) *AFD1* (Golubovskaya *et al.*, 2006) and rice (*Oryza sativa*) *OsRAD21-4* (Zhang *et al.*, 2006b), result in defects in chromosome condensation, subsequent pairing and synapsis and separation of chromatids. After the pre-meiosis replication and the formation of SCC, homolog recognition, pairing and recombination take place during the extended meiotic prophase I (Hamant *et al.*, 2006). The mechanism of homolog recognition and pairing is still poorly understood. In a wide range of species the telomeres cluster together in early meiotic prophase to form a structure called the telomere

bouquet (Bass *et al.*, 1997; Rockmill and Roeder, 1998; Scherthan, 2001). This structure, together with the centromere association found in several species (Martinez-Perez *et al.*, 2001; Tsubouchi and Roeder, 2005), is thought to facilitate the initial contacts that lead to homologous pairing (Ma, 2006). Double-strand breaks (DSBs) introduced by Spo11 lead to a DSB-dependent recombination process (Bergerat *et al.*, 1997). Accumulating data from many eukaryotes show that the formation of DSBs is required for synapsis (Keeney, 2001), a process that forms an intimate and stable interaction between the chromosome arms by a structure called the synaptonemal complex (SC). Mutations of the SC genes usually result in defects in homologous pairing, synapsis and univalent formation. Examples of such genes include *ASY1* of Arabidopsis (Caryl *et al.*, 2000; Armstrong *et al.*, 2002) and *PAIR2* of rice (Nonomura *et al.*, 2004b, 2006), orthologs to yeast *HOP1* (Hollingsworth *et al.*, 1990), functioning in the lateral elements of the SC. Knockdown of the *AtZYP1*, a homolog of yeast *ZYP1* functioning in the central element of the SC (Sym *et al.*, 1993), results in delayed meiosis, absence of pairing, and synapsis in most meiocytes (Higgins *et al.*, 2005).

With the completion of the rice genome sequence and the production of libraries of tagged mutants, the stage is now set for the identification of novel genes involved in meiosis in rice. Nonomura *et al.* (2004a) identified a mutant of the *PAIR1* gene encoding a putative coiled-coil protein from a *TOS17* mutant library. During prophase I, the chromosomes in the meiocytes of the *pair1* mutant become entangled to form a compact sphere adhering to the nucleolus and homologous pairing fails. Another example is *PAIR2*, an ortholog of *Saccharomyces cerevisiae HOP1* (Hollingsworth *et al.*, 1990) and Arabidopsis *ASY1* (Caryl *et al.*, 2000; Armstrong *et al.*, 2002), which is required for homologous chromosome synapsis in meiosis I (Nonomura *et al.*, 2004b, 2006).

In order to elucidate the genetic and molecular control of the process of meiosis in rice, more mutants and the corresponding genes need to be characterized to provide knowledge for systematic construction of this process. Here, we report the characterization of a novel meiotic gene *PAIR3* (*HOMOLOGOUS PAIRING ABERRATION IN RICE MEIOSIS 3*), encoding a putative coiled-coil protein in rice. Two individual T-DNA insertion lines, *pair3-1* and *pair3-2*, exhibit male and female sterility. During meiotic prophase I, both mutants fail in homologous chromosome pairing and synapsis, resulting in no formation of bivalents and subsequent random segregation of the univalents in anaphase I. The *pair3* mutants produce defective pollen and megaspores. Our molecular studies on PAIR3 have not found any indication of a physical or regulatory association between PAIR3 and PAIR1, indicating that PAIR3 may have a distinct function in rice chromosome pairing.

RESULTS

Identification of the *pair3* mutant in rice

We previously generated a population of rice T-DNA insertion mutants by adopting the GAL4/VP16-UAS enhancer trap system (Wu *et al.*, 2003; Zhang *et al.*, 2006a). In order to identify genes that are involved in the process of meiosis in rice, large-scale screening for sterile mutant lines was carried out. A total of 2000 independent T_1 families were planted in the field during the rice-growing season of 2004 under normal field growth conditions in Wuhan, China, with 20 plants per family. We identified 30 lines in which partial or complete sterility segregated as a single recessive mutation. We carried out a detailed study of mutant line 03Z11UF78 showing complete sterility. The segregation ratio in the T_1 family of 20 plants (fertile:sterile = 14:6, $\chi^2 = 0.238$ for 3:1) suggested that the sterility phenotype was caused by a recessive mutation of a single Mendelian locus that was controlled sporophytically. The mutant plants (155 examined) exhibited normal phenotype except that they failed to produce any seed or release any pollen (Figure 1a–c). The anther showed a pale-yellow color (Figure 1d,e), and almost all the pollen lacked starch, as revealed by iodium potassium iodide staining (Figure 1f,g). Pollinating the flowers of 20 panicles from the mutant with wild-type (WT) pollen did not produce seed, suggesting that both male and female gametes were almost completely abortive.

T-DNA insertion caused the *pair3* mutant phenotype

The genomic fragment flanking the T-DNA insertion site was isolated from the *pair3* mutant plant using thermal asymmetric interlaced (TAIL)-PCR (Zhang *et al.*, 2007). A BLASTn search of the T-DNA flanking sequence against the genomic sequence (http://rice.plantbiology.msu.edu/) showed that the T-DNA was inserted into a putative gene (LOC_Os10g26560) located on chromosome 10, annotated as a hypothetical protein with no close homologs in other species. This gene consisted of 11 exons and the T-DNA insertion site was 620 bp upstream of the ATG start codon (Figure 2a).

To test whether the sterile mutant phenotype was due to T-DNA insertion in the LOC_Os10g26560 locus, we determined the genotypes of T_1 plants by PCR amplification of the T-DNA insertion site using the primers a, b and c (Figure 2a). Among 20 T_1 plants, the six plants showing complete sterility were homozygous for the T-DNA insertion, while the other plants, either hemizygous or homozygous for WT, exhibited normal fertility (Figure 2b). Twenty T_2 plants from each WT T_1 segregant (lines 1, 2, 6, 11, 14 and 18) and 40 T_2 plants derived from each hemizygous T_1 segregant (lines 3, 5, 9, 12, 13, 16 and 17) were further assayed by PCR for co-segregation between the *pair3* allele and sterility. All the progeny from WT plants exhibited normal fertility, and all the T-DNA insertion homozygotes in each family of the 40

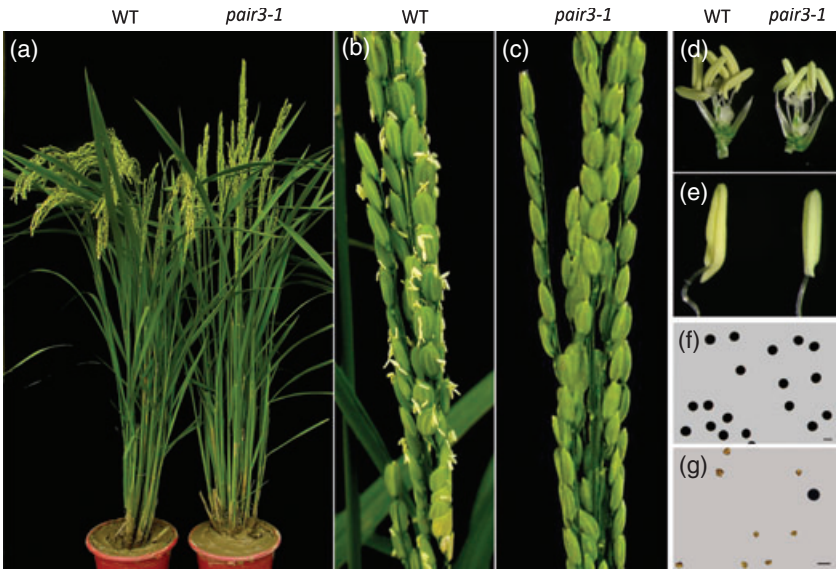

Figure 1. Comparison of the wild type (WT) and the *pair3-1* mutant at the heading stage.
(a) WT plant (left) and a *pair3-1* mutant plant (right). (b) A panicle from a WT plant. (c) A panicle from the *pair3-1* mutant. (d) Florets from a WT (left) and a *pair3-1* (right) plants. (e) Anthers from a WT (left) and a *pair3-1* (right) plants. (f) Fertile pollen of a WT plant, stained by iodium potassium iodide solution. (g) Sterile pollen in the homozygous *pair3-1* mutant. Bar = 50 μm.

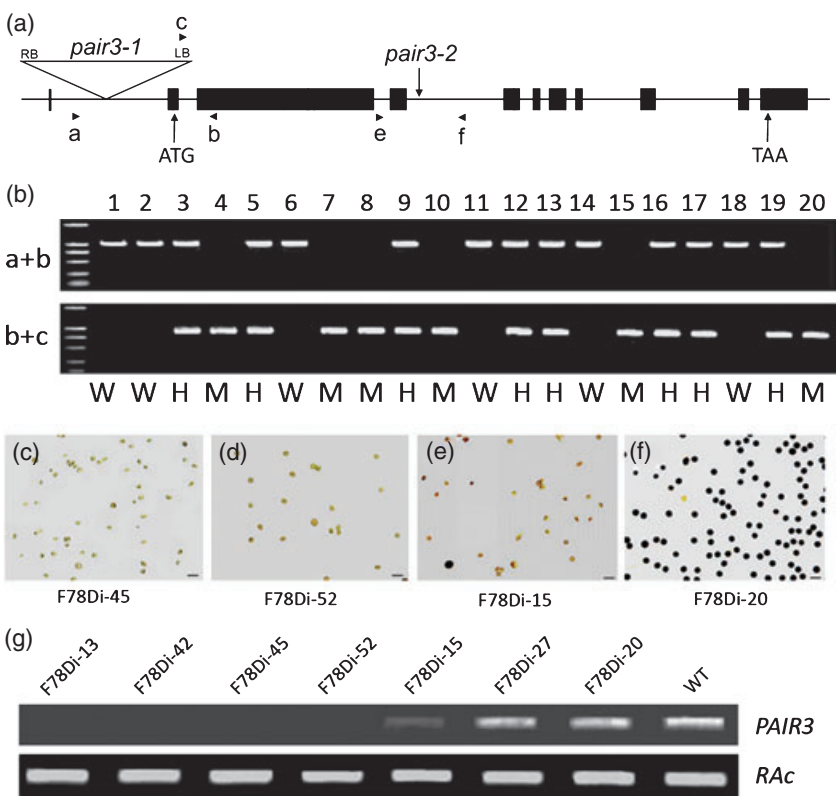

Figure 2. A schematic diagram of *PAIR3*, position of the T-DNA insertion, genotyping of the *pair3-1* progeny and RNAi transgenic analysis. (a) Structure of *PAIR3* and the T-DNA insertion site. Eleven exons (boxes) and 10 introns (lines between boxes) are shown. The vertical arrows indicate the ATG start codon and TAA stop codon. T-DNA insertion sites of *pair3-1* and *pair3-2* were located in the first and the fourth introns, respectively. Arrowheads indicate the positions and orientations of the PCR primers: a, b, c, e, f used to genotype the T_1 and T_2 plants. RB, right border; LB, left border of the T-DNA. (b) The PCR genotyping of the *pair3-1* segregants. Samples 1, 2, 6, 11, 14 and 18, which show normal phenotype amplified only the genomic DNA (a + b) and therefore are wild type (W); Samples 4, 7, 8, 10 and 15, which are completely sterile amplified only the 0.9-kb band (b + c) and are therefore homozygous (M); the other samples amplified both bands and are heterozygous (H), and show normal phenotype. (c)–(f) Pollen: (c) sterile pollen in the F78Di-45 transgenic line; (d) sterile pollen in the F78Di-52 transgenic line; (e) partly sterile pollen in the F78Di-15 transgenic line; (f) fertile pollen in the transgene-negative line (F78Di-20). Bar = 25 μm. (g) Transcript levels of *PAIR3* RNAi plants. *PAIR3* transcript levels were examined by semi-quantitative RT-PCR using F78RT4 primers. Rice *actin* (*RAc*) was used as a control.

plants were completely sterile (result not shown), indicating a perfect co-segregation between T-DNA insertion and fertility. These results strongly suggested that the sterile mutant phenotype was caused by the T-DNA insertion in LOC_Os10g26560 or a very closely linked lesion. We named this gene *PAIR3* and this mutant *pair3-1*.

To substantiate the result, we searched our rice T-DNA flanking sequence database (http://rmd.ncpgr.cn/; Zhang *et al.*, 2006a) using the *PAIR3* sequence and found an allelic mutant 05Z11HE71, which we named *pair3-2*. The T-DNA insertion site was located in the fourth intron of LOC_Os10g26560 (Figure 2a). The *pair3-2* mutant also showed a complete male and female sterile phenotype (Figure S1a–f in Supporting Information). Genotyping by PCR confirmed that the sterility co-segregated with the T-DNA insertion in the *PAIR3* locus (Figure S1g).

RNAi plants of *PAIR3* phenocopied the T-DNA insertional mutants

To further verify that the male and female sterile phenotype was attributable to the loss of function of *PAIR3*, we generated transgenic plants that suppressed the expression of *PAIR3* by RNAi. A 392-bp fragment in the third exon of *PAIR3* was amplified and cloned to the pDS1301 vector (under the control of cauliflower mosaic virus 35S promoter) with an inverted repeat through restriction enzyme digestion (Yuan *et al.*, 2007). The construct was introduced into the rice variety Zhonghua 11 by the *Agrobacterium tumefaciens*-mediated transformation method (Wu *et al.*, 2003). Of 52 positive transgenic plants, 21 produced empty seeds and sterile pollen (Figure 2c,d), and nine transgenic plants showed partial sterility (Figure 2e), while the remaining 22 transgene-positive and eight transgene-negative plants exhibited normal fertility (spikelet fertility >50%) (Figure 2f). The abundance of *PAIR3* transcripts in RNAi plants was examined using RT-PCR. In completely sterile RNAi plants (F78Di-13, 42, 45 and 52) the *PAIR3* transcript was undetectable, whereas the partially sterile plants (F78Di-15) had a *PAIR3* transcript level that was readily detectable, but less than that in the fertile plants from positive (F78Di-27) or negative (F78Di-20) transformants (Figure 2g). Based on the above data, we concluded that mutation in *PAIR3* was the cause for the sterile phenotype in both male and female gametophytes.

PAIR3 is a novel gene encoding a coiled-coil protein in rice

The predicted coding sequence of *PAIR3* is 2442 bp according to the annotation in the TIGR database (http://rice.plantbiology.msu.edu/index.shtml). Rapid amplification of the cDNA ends (RACE) and RT-PCR amplification were performed to characterize the full-length *PAIR3* transcript. The RT-PCR result indicated that there were two differences compared with the predicted structure. One was that the predicted second intron did not exist and the other was that the predicted fifth exon should have been 51 bp longer at the 3′-end. Alignment of the transcript with the genomic sequence of the WT variety Zhonghua 11 (the same as that of Nipponbare) showed that the *PAIR3* transcript consisted of 11 exons, interrupted by 10 introns (Figure 2a), which were spliced out at canonical GT–AG sites. The length of the 5′-untranslated region (UTR) was 62 bp, spanning the first two exons, and the 3′-UTR length was 366 bp (Figure 3a).

The deduced PAIR3 protein is 844 amino acids in length (Figure 3b). A BLASTp search of the predicted PAIR3 protein against the non-redundant sequence protein database (http://www.ncbi.nlm.nih.gov/) failed to retrieve any known functional protein with high similarity, indicating that the peptide sequence of PAIR3 is poorly conserved. Online

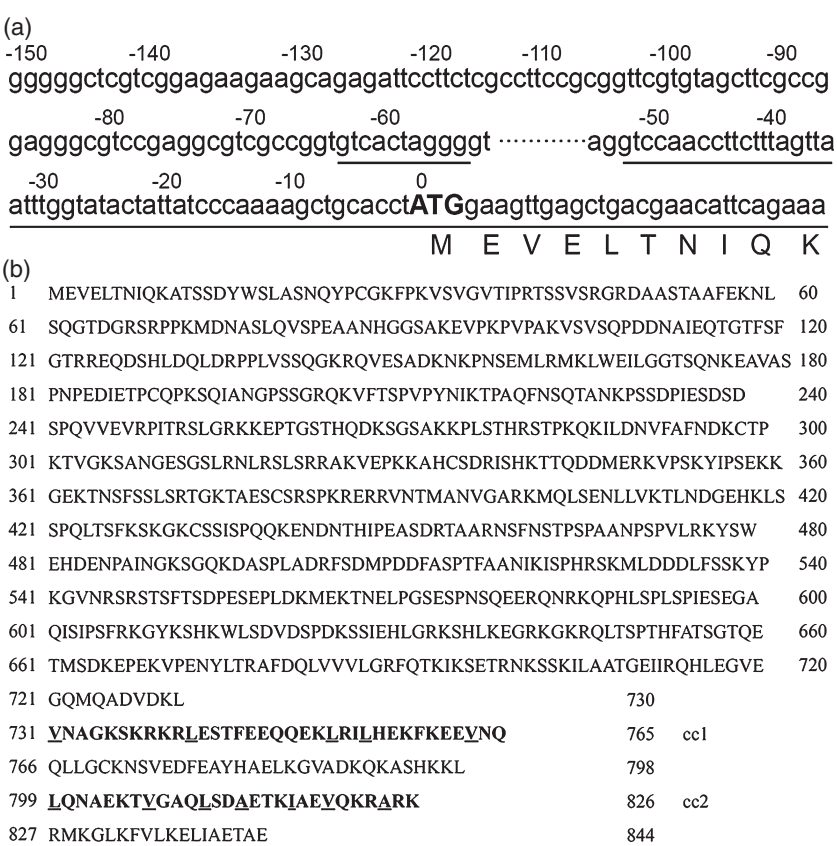

Figure 3. Identification and structure prediction of the *PAIR3* gene.
(a) Genomic sequence upstream of the *PAIR3* coding region. Underlining indicates the 5′-untranslated (UTR) end predicted by 5′ rapid amplification of the cDNA ends (RACE) and the translation initial codon ATG is in bold.
(b) The deduced amino acid sequence of PAIR3. The coiled-coil structure with two heptad clusters (cc1 and cc2) is predicted at the end of peptide (marked in bold). The first and fourth residues in heptad repeats are frequently hydrophobic (underlined).

network protein sequence analysis (Combet *et al.*, 2000) predicted two α-helical coiled-coil motifs with nine heptad repeats, both of which were located near the C-terminus of the peptide [731–765 amino acids (cc1), 799–826 amino acids (cc2)] of PAIR3.

Abnormal male and female gametophyte formation in *pair3* mutants

To characterize the male and female sterility of the *pair3* mutants, we compared the development of the anther and embryo sac in the WT and *pair3-1* mutant by histological examination of plastic or paraffin transverse sections.

Rice anther development was delineated into eight stages according to previous classifications (Feng *et al.*, 2001; Jung *et al.*, 2005, 2006; Li *et al.*, 2006). Compared with WT, there was no obvious difference in *pair3-1* during the early pre-meiosis stage (Figure 4a,b) and the microspore mother cell stage (Figure 4c,d). The mutant phenotype of *pair3-1* was observed at the meiosis stage (Figure 4e,f) and the tetrad stage (Figure 4g,h), in which the microsporocytes, tetrads and uninucleate microspores were larger (Figure 4f,h,i,j), more irregularly shaped and less dense in cytoplasmic staining. Subsequently, at the vacuolated pollen stage, the vacuolated pollen defaulted in cell wall thickening and cell solute accumulation in *pair3-1* (Figure 4k,l). At the pollen mitosis stage (Figure 4m,n) and mature pollen stage (Figure 4o,p), the *pair3-1* pollen grains severely collapsed and consequently no normal pollen grains were released. These findings suggest that PAIR3 functions during meiosis in male gamete formation. Although PAIR3 is not required for tetrad formation as such, it is essential for normal development of the resulting microspores.

The process of development of the rice embryo sac was divided into eight stages as described previously (Liu *et al.*, 1997). A single subdermal nucellar cell, called the archesporium, enlarged and displayed a prominent nucleus at archesporial cell formation (Figure 5a,b) and the single cell elongated and developed directly into the megaspore mother cell (Figure 5c,d). During the megasporocyte meiosis stage (Figure 5e,f), the megasporocyte underwent two successive meiotic divisions and formed a linear array of megaspores along the micropylar–chalazal axis. Subsequently, the megaspore nearest the chalaza enlarged, and the three other megaspores degenerated and were crushed by the enlarging megaspore at the functional megaspore formation stage (Figure 5g). The WT functional megaspore elongated and enlarged again and formed a uninucleate embryo sac (Figure 5i), which initiated haploid mitosis (Figure 5k). Three rounds of haploid mitosis produced the eight-nucleate mature embryo sac (Figure 5m). This structure contained seven cells: three antipodal cells, one central cell, two synergid cells and one egg cell (Figure 5o). Compared with the WT, no abnormality was detected in *pair3-1* in the first three stages (Figure 5b,d,f). However, at the functional megaspore formation stage, the degeneration of the three non-functional megaspores was not followed in *pair3* by the enlargement of the surviving megaspore because it was also degenerated (Figure 5h). Subsequently, traces of the degenerating megaspores persisted for a long time in *pair3-1* (Figure 5j) and *pair3-2* (Figure 5l) mutants and the embryo sac was replaced by remnants of degenerated nucellus in *pair3-1* (Figure 5n) and *pair3-2* (Figure 5p) (>20 ovules examined). These observations demonstrated that the *pair3* mutations caused defects in functional megaspore formation and, as a result, in embryo sac formation.

Failure of bivalent formation at diakinesis in *pair3* meiocytes

In order to further investigate the cause of male sterility in *pair3* mutants, we compared chromosomal behavior during meiosis in pollen mother cells of the WT and the *pair3* mutants. In the WT, the chromosomes began to condense and appeared very thin at leptotene (Figure 6a) and homologous chromosome underwent pairing and synapsis at zygotene (Figure 6c). At pachytene, homologous chromosomes are fully synapsed with the completion of the SC (Figure 6e). Up to the diplotene stage (Figure 6g), the SCs were disassembled and the homologous chromosomes separated from one another except at the chiasmata. At diakinesis (Figures 6i and S2a), chromosomes further condensed to produce very short chromosomal pairs, seen as 12 bivalents. The bivalents aligned themselves along the equatorial plane at metaphase I (Figures 6k and S2c), after which the homologous chromosome separated reductionally and moved to the two poles of the cell at anaphase I (Figures 6m and S2e). After meiosis I, two groups of chromosomes were aligned separately at two new division planes. Next the sister chromosomes separated equationally through meiosis II and produced tetrad spores (Figures 6o and S2g).

In the *pair3-1* mutants, the chromosomes began to condense at leptotene (Figure 6m) but failed to form a compact sphere adhered to the nucleolus and did not produce the synizetic knot at zygotene (Figure 6d; arrow indicates synizetic knot at Figure 6c). After zygotene (so-called pachytene-like) the chromosomes continued to condense, whereas the chromosomes were comparatively thinner and showed more lines compared with WT, indicating non-synaptic chromosomes, and no obvious pachytene existed in the *pair3-1* mutant (Figure 6f). Up to diplotene, thin threads still aggregated together (Figure 6h). The most obvious defects were found at diakinesis: (i) all of the cells checked (>200 cells) had >12 but ≤24 univalents in the *pair3-1* and *pair3-2* mutant meiocytes (Figures 6j and S2b), and (ii) the univalents showed no chromatin bridges, and no chromosome fragments were detected. Subsequently all the univalents aggregated at the equatorial plane at metaphase I (Figures 6l and S2d) and the univalents randomly segregated to the two poles at anaphase I (cell: $n = 200$),

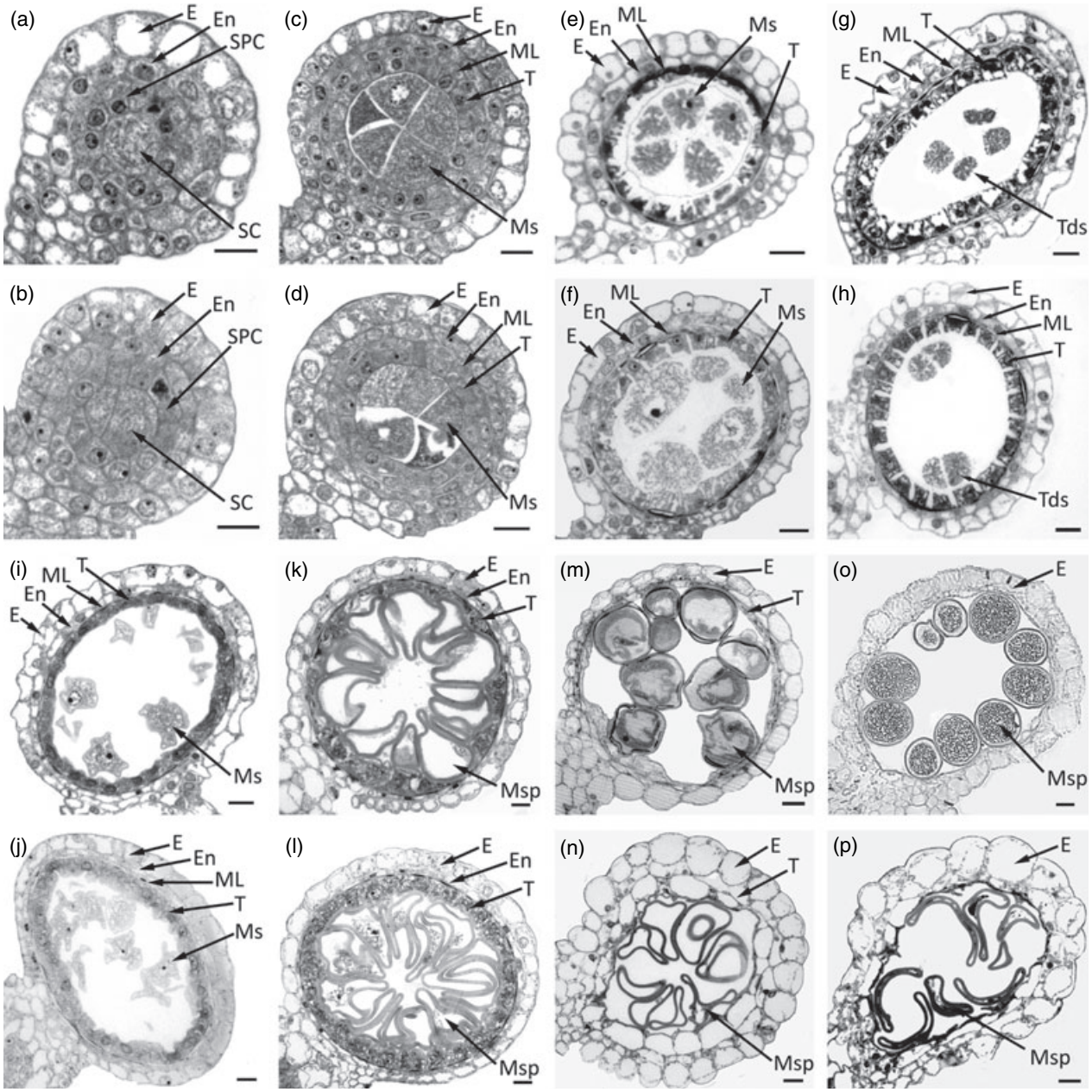

Figure 4. Transverse section analysis of the anther development of the wild type (WT) and the *pair3-1* mutant.
Cross sections of WT (a, c, e, g, i, k, m, o) and *pair3-1* (b, d, f, h, j, l, n, p) at the early pre-meiosis stage (a, b), microspore mother cell stage (c, d), meiosis stage (e, f), tetrad stage (g, h), young microspore stage (i, j), vacuolated pollen stage (k, l), pollen mitosis stage (m, n), and mature pollen stage (o, p). E, epidermis; En, endothecium; ML, middle layer; T, tapetum; Ms, microsporocyte; Tds, tetrads; Msp, microspore; MP, mature pollen; SPC, secondary parietal cell; SC, sporogenous cell. Bars = 25 μm.

frequently with unequal numbers of chromosomes at two poles (Figure 6n) or with lagging of univalent separation morphologies (Figure S2f). Despite an unequal division of univalents between dyads and tetrads in *pair3*, cytokinesis of meiocytes seemed normal for the formation of tetrads (Figures 6p and S2h). We concluded that the loss-of-function of the *PAIR3* gene affected normal chromosome pairing and synapsis and subsequently univalents segregated randomly in meiosis I in male meiocytes, leading to almost completely sterile pollen in the *pair3* mutants.

PAIR3 transcript is abundant in meiocytes during meiosis

To examine the *PAIR3* expression pattern, we conducted RT-PCR assays on total RNAs extracted from root, stem, leaf sheath, leaf blade and developing panicles. Accumulation of *PAIR3* transcripts was observed in young panicles at a very

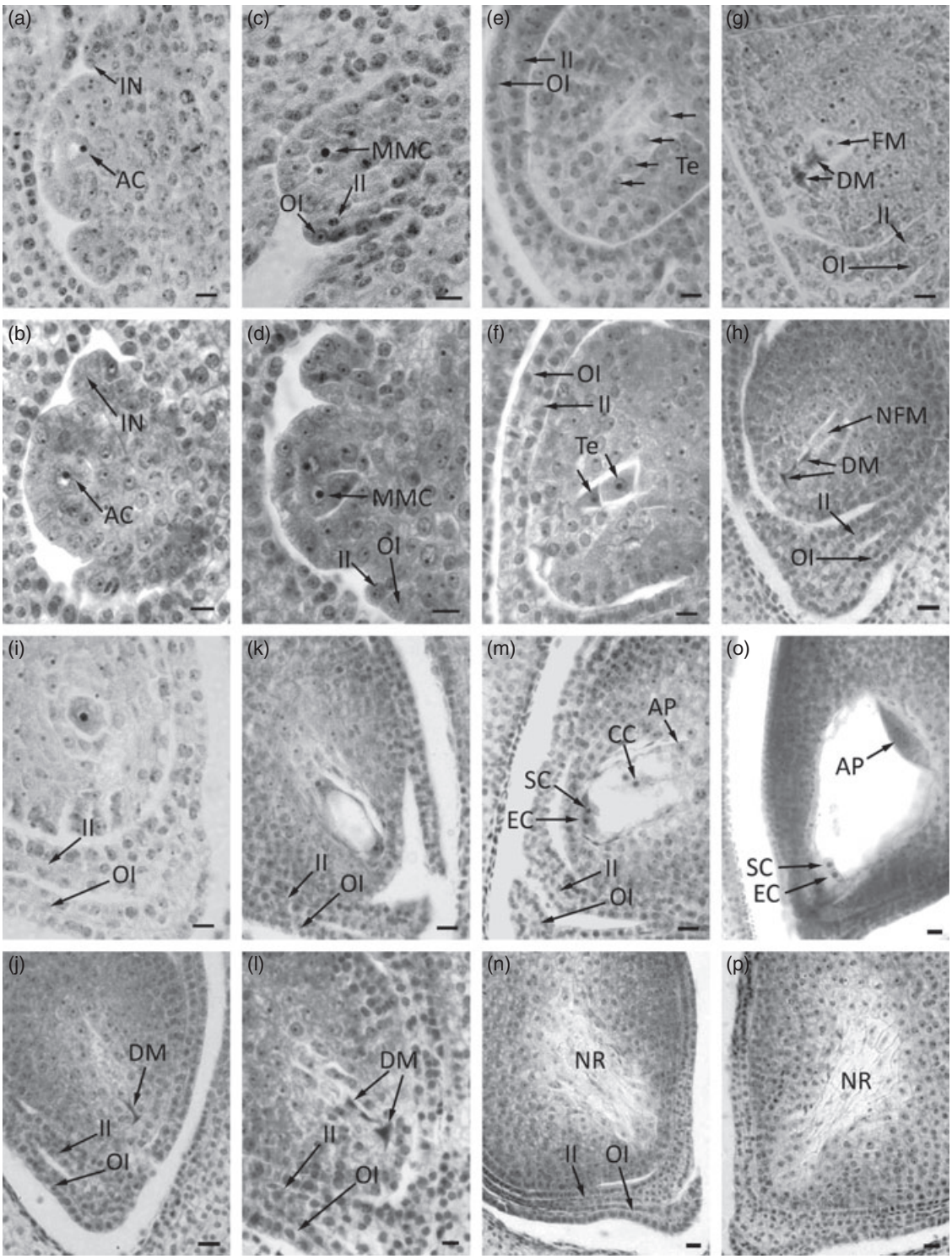

Figure 5. Transverse section analysis of embryo sac development in the WT and the *pair3* mutants.
Cross sections of WT (a, c, e, g, i, k, m, o) and *pair3* (b, d, f, h, j, l, n, p) at the archesporial cell formation stage (a, b), megasporocyte formation stage (c, d), megasporocyte meiosis stage (e, f), functional megaspore formation stage (g, h), mononucleate embryo sac formation stage (i), embryo sac mitosis stage (k), eight-nucleate embryo sac developing stage (m), mature embryo sac stage (o). Parts (j) and (n) show that the so-called functional megaspore degenerated following the other three megaspore in the *pair3-1* and *pair3-2* mutant respectively. Parts (l) and (p) show no embryo sac formation in the *pair3-1* and *pair3-2* mutants, respectively, at a later stage. AC, archesporial cell; IN, integument primordium; MMC, megaspore mother cell; OI, outer integument; II, inner integument; Te, tetrad; FM, functional megaspore; DM, degenerated megaspore; NFM, non-functional megaspore; NR, nucellar remnants; AP, antipodals; CC, central cell; EC, egg cell; SC, synergid cell. Bars = 10 μm.

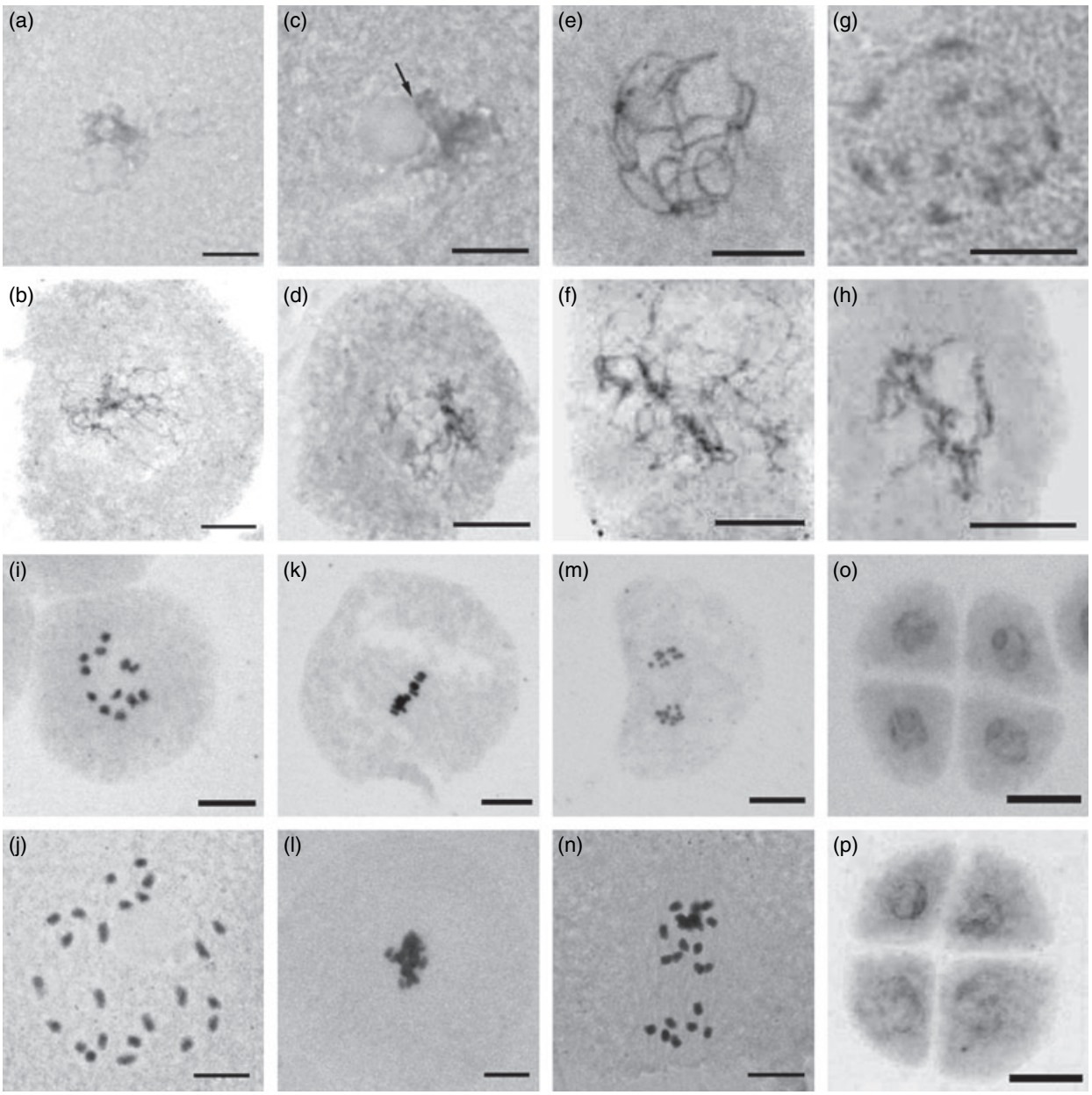

Figure 6. Male meiocyte meiosis analysis of the wild type (WT) and the *pair3-1* mutant.
Chromosome behavior of male meiocytes of the WT (a, c, e, g, i, k, m, o) and *pair3-1* (b, d, f, h, j, l, n, p) at various stages: leptotene (a, b); zygotene (c, d), arrow indicates the synizetic knot; pachytene (e) and pachytene-like (f); diplotene (g, h); diakinesis (i, j); metaphase I (k, l); anaphase I (m, n); tetrad spore (o, p). Homologous chromosome pairing and synapsis are defective and 24 complete univalents are observed in *pair3-1* pollen at diakinesis (j), and subsequently the univalents are randomly divided at anaphase I (n). Bar = 10 μm.

Figure 7. Expression patterns of *PAIR3* by semi-quantitative RT-PCR and *in situ* hybridization analysis. (a) The RT-PCR analysis of the expression pattern of *PAIR3* in sheath, leaf and panicle from wild type (WT) and mutant plants at the booting stage. *RAc* is used as a control for mRNA levels. (b) Expression patterns of the *PAIR3* gene in panicles. All the vegetative tissues were collected from booting plants. R, root, S, stem, Sh, leaf sheath; L, leaf; P1, approximately 0.5 cm; P2, approximately 1.0 cm; P3, approximately 2.0 cm; P4, approximately 3.5 cm; P5, approximately 4.5 cm, P8, approximately 11 cm; P9, approximately 16.5 cm; P10, approximately 19 cm; P11, approximately 22 cm; MP, panicles of approximately 18-cm length from mutant plants; G, genomic DNA. The numbers on the right indicate the PCR cycles. (c–h) *In situ* analysis of *PAIR3* expression patterns in different stages of anther development: the early pre-meiosis stage (c); the late meiosis stage (d); the early young microspore stage (e); the late young microspore stage (f); the vacuolated pollen stage (g); and the pollen mitosis stage (h). (i–m) *In situ* hybridization analysis of *PAIR3* expression patterns in different stages of embryo sac development: the megasporocyte formation stage (i); the functional megaspore formation stage (j); the mononucleate embryo sac formation stage (k); the embryo sac mitosis stage (l); the mature embryo sac stage (m). (n, o) Negative control for the pollen and embryo sac respectively. SPC, secondary parietal cell; SC, sporogenous cell; Ms, microsporocyte; Tds, tetrad; Msp, microspore; T, tapetum; MMC, megaspore mother cell; II, inner integument; OI, outer integument; IN, integument; NU, nucellus; FU, funiculus; AP, antipodals. Bar = 25 μm.

low level in vegetative organs (Figure 7a). The *PAIR3* transcripts were repressed greatly in the young panicles of *pair3-1* (Figure 7a) and *pair3-2* mutants (Figure S3), confirming their status as loss-of-function mutants. In order to further determine *PAIR3* expression patterns in various stages of panicle development, RT-PCR was conducted on total RNA from different young panicle sizes (0.5–19 cm). *PAIR3* transcripts were detected at a low level in P1 (approximately 0.5 cm) panicles, reached a peak abundance in P5 (approximately 4.5 cm) panicles, and then decreased to

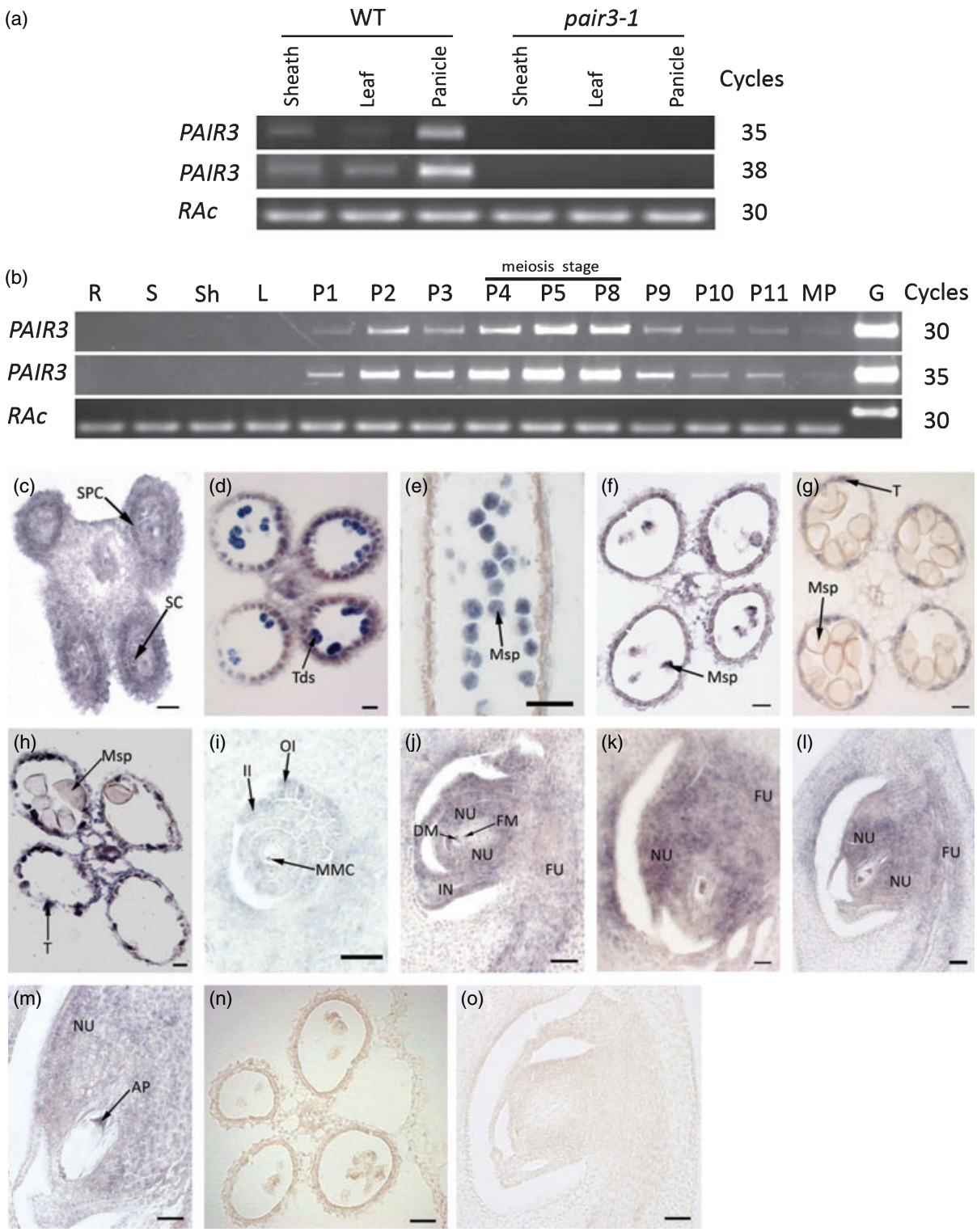

a very low level in mature panicles (Figure 7b). It has been reported that meiocytes undergo meiosis from P4 (approximately 3.5 cm) to P8 (approximately 11 cm) in rice (Nonomura *et al.*, 2004a,b). Thus, *PAIR3* expression is greatest around the time of meiosis.

To determine more precisely the spatial and temporal expression pattern of *PAIR3* during the meiocyte meiosis, we carried out RNA *in situ* hybridization with WT floral sections. The RNA *in situ* hybridization signals were first detected in the microsporogenous cells and the primordial cells of the parietal layers at the pre-meiosis stage (Figure 7c). Subsequently, the signals were detected exclusively in the meiocytes, dyads, tetrads (Figure 7d) and the early young microspores (Figure 7e), but were undetectable in the parietal cells of the anther (Figure 7d,e). In the later young microspores, the *PAIR3* signal was reduced to a lower level (Figure 7f). The *PAIR3* signal was absent from vacuolated pollen, mitotic pollen and mature pollen, but a strong signal was detected in the degenerating tapetum (Figure 7g,h). We also performed RNA *in situ* hybridization in the ovule tissues during embryo sac development. *PAIR3* expression was detected in all the ovule tissues including the integument, nucellus, funiculus, embryo sac and the inner layer cells of the carpel wall during embryo sac development (Figure 7i–m). The signal was very high during or just after the megasporocyte meiosis stage (Figure 7j,k,l). Although RNA *in situ* hybridization was not a method of choice for quantification, the relative expression levels could still be gauged by the stain intensity. The expression pattern of *PAIR3* from *in situ* hybridization corresponded well with the RT-PCR results. The *PAIR3* gene was preferentially expressed in the meiocytes, especially during the male and female meiosis stages. The expression pattern of *PAIR3* together with the phenotype observed in the loss-of-function mutants indicated that the PAIR3 protein works in the meiocytes and plays crucial roles in homologous pairing and synapsis.

The PAIR3 mutations do not affect the expression of other rice meiotic genes

A recent review summarized progress in the identification of meiosis-related genes in plant species (Mercier and Grelon, 2008). Five genes (*PAIR1*, *PAIR2*, *MEL1*, *OsDMC1* and *OsRad21-4*) have been characterized for function in meiosis in rice (Nonomura *et al.*, 2004a,b; Nonomura *et al.*, 2007; Zhang *et al.*, 2006b; Deng and Wang, 2007) and all of them are expressed during or before/after meiosis as judged by developmental stages based on panicle length. We compared the expression of these five genes and *PAIR3* in WT and *pair3-1* during meiosis. Their transcription levels were not obviously affected in the *pair3-1* mutant (Figure 8), indicating that expression of these five genes is likely to be independent of *PAIR3* function in controlling chromosome pairing during meiosis.

DISCUSSION

PAIR3 functions in gametophyte development

The *pair3* mutants showed complete male and female sterility due to failure of gametophyte development. Based on the histological studies of male gametophyte development (Figure 4) and evidence of *PAIR3* gene expression in most of the meiocytes during male meiosis (Figure 7d), we concluded that *PAIR3* functions in male meiosis. The cells of the parietal layer including the tapetum appeared to be normal, indicating that *PAIR3* did not function in anther wall development and that the male sterile mutant phenotype was not due to defects in anther wall development. This is different from the situation frequently reported in the literature in which male sterility is often associated with defects in tapetum development (Jung *et al.*, 2005; Li *et al.*, 2006). Although the *PAIR3* gene was highly expressed in the degenerating tapetum, there was no obvious difference in the tapetum of the *pair3* mutants (Figure 4) compared with that of WT, indicating that PAIR3 may not function in tapetal degeneration. From the histological studies of female gametophyte development (Figure 5), ovule development seemed normal, although *PAIR3* was expressed strongly in the whole ovule (Figure 7j,k,l). The first ovular defect was observed at the functional megaspore formation stage, when the megaspore near the chalaza was degenerated along with the other three degenerating megaspores nearer the micropyle (Figure 5j,l). Subsequently, no embryo sac structure appeared in the mutant ovary (Figure 5n,p).

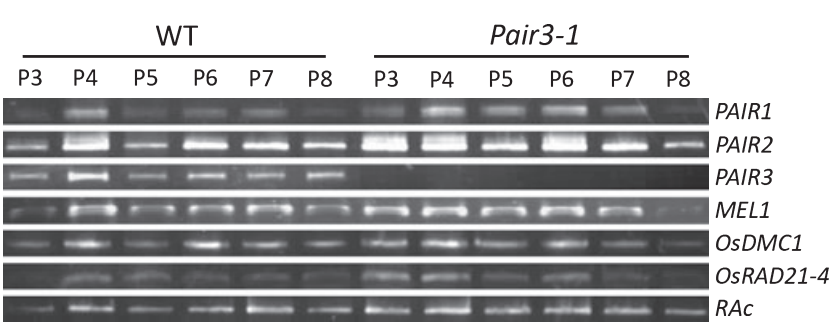

Figure 8. Semi-quantitative RT-PCR analyses of rice genes related to meiosis in the inflorescence of the wild type (WT) and *pair3-1* mutant.
Panicles of length P3, approximately 2.0 cm; P4, approximately 3.5 cm; P5, approximately 4.5 cm, P6, approximately 6 cm; P7, approximately 8 cm; P8, approximately 11 cm were prepared for isolation RNA from WT and *pair3-1*, respectively.

PAIR3 is required for pairing but not cytokinesis

The formation of univalents at diakinesis (Figures 6j and S2b) in the *pair3* mutants suggested synapsis defects, which can be classified into two categories, asynapsis and desynapsis (Ma, 2005). Asynapsis mutants are characterized by partial or complete failure of synapsis and the lack of chiasmata structures, while desynapsis is caused by the lesion in the SC and represents segregation of the chiasmata structure. The thinner chromatin threads and more lines (Figure 6f) shown at pachytene-like of the *pair3* mutant might represent the lack of SC structure and a failure of synapsis, suggesting that *pair3* may be an asynaptic mutant. The *pair3* asynaptic phenotype may be caused either by a defect of the SC, as in *asy1* of Arabidopsis and *pair2* of rice, or by defects of other processes, such as DSB dependent recombination (Stacey *et al.*, 2006), that are closely linked to synapsis. Immunocytological localization of the PAIR3 protein will be carried out in a future study, and should help to determine the roles of PAIR3 in pairing and synapsis. It should also be noted that although the segregation of univalents at anaphase I was abnormal in the *pair3* mutant (Figures 6n and S2f), the subsequent cytokinesis division appeared normal and resulted in only tetrads. This suggests that PAIR3 is dispensable for normal cytokinesis in rice.

Functional comparison of *PAIR1*, *PAIR2* and *PAIR3*

Both *pair1* and *pair2* mutants showed 24 completely unpaired univalents at diakinesis, and both the male and female meiocytes were affected, causing complete male and female sterility (Nonomura *et al.*, 2004a,b). The *pair3* mutants showed similar effects but there were some important differences. Whereas the *pair1* and *pair2* mutants showed abnormalities in cytokinesis in meiocytes, with production of dyads as well as tetrads, the *pair3* mutant produced only tetrads and microsporocytes after meiosis. *PAIR1* expression occurred in the early stages of meiosis, whereas *PAIR2* and *PAIR3* were expressed in all stages of anther development. As *pair1* was reported to lack an embryo sac structure in the ovule (Nonomura *et al.*, 2004a), we speculate that homologous chromosome pairing and synapsis also failed in the megaspore mother cells, and that degeneration of the megaspore and the absence of an embryo sac in *pair3* mutants were secondary effects of defective chromosome pairing.

PAIR3 showed no strong similarity with any known proteins and had no known motifs except the coiled-coil domain. Coiled-coil domains have been found in a large class of proteins. It is estimated that approximately 10% of all proteins contain coiled-coil domains (Liu and Rost, 2001). These domains can facilitate protein–protein interactions by forming homodimers and/or heterodimers (Lupas, 1996). We speculate that PAIR3 may form a coiled-coil dimer and/or interact with another protein to act on chromosomes during meiosis. Indeed, the SCs are known to be composed of many coiled-coil proteins (Hirano, 2000). In addition, the SWI1 and PAIR1 proteins, required for normal bivalent formation at meiosis, also contain a putative coiled-coil structure (Mercier *et al.*, 2001; Nonomura *et al.*, 2004a). We performed a yeast two-hybrid assay for possible interaction of the coiled-coil domains between PAIR1 and PAIR3, but did not detect interaction between the two proteins (data not shown). Thus PAIR1 and PAIR3 might contribute to distinct protein complexes for homologous pairing and synapsis in meiosis.

EXPERIMENTAL PROCEDURES

Plant materials and growth conditions

Callus derived from mature embryos of the rice *japonica* cultivar Zhonghua 11 was employed to create T_0 generation mutants by the *A. tumefaciens* mediated transformation method (Wu *et al.*, 2003), and T_1 families of the mutants were planted in the experimental field of Huazhong Agriculture University at Wuhan, China, in the summer of 2004 (latitude 30.5°N, 15 m above sea level; average daily temperature approximately 28°C). The *pair3-1* mutant showing complete sterility was identified by screening. The *pair3-2* mutant was obtained by searching our T-DNA insertion mutant library using the *PAIR3* sequence. The mutant lines described in this article can be accessed and are available at the National Center of Plant Gene Research (Wuhan), Huazhong Agricultural University, China (http://rmd.ncpgr.cn/).

Genotyping of mutant plants

The DNA extraction and flanking sequence isolation were performed as described by Zhang *et al.* (2007). A rice genomic sequence corresponding to the T-DNA flanking sequence was identified using BLASTN on the Institute for Genomic Research database (http://rice.plantbiology.msu.edu/blast.shtml). The co-segregation relationship between the sterile phenotype and the T-DNA homozygous insertion was analyzed by PCR in the T_1 and T_2 populations. The PCR genotyping for the *pair3* segregation families was performed using a set of primers (Figure 2a, Table S1): a, b and c for the *pair3-1* allele, and e, f ands c for the *pair3-2* allele, respectively. The PCR conditions were: an initial step of 94°C incubation for 5 min followed by 30 cycles of 94°C for 45 sec, 55°C for 45 sec and 72°C for 1 min.

Determining the full-length transcripts

Total RNA was isolated from young panicles (approximately 4.0–6.0 cm) using TRIzol reagent (Invitrogen, http://www.invitrogen.com/) according to the manufacturer's instructions. The cDNA synthesis was performed by 5′-RACE and 3′-RACE using the SMART® RACE cDNA amplification kit (Takara Bio, Clontech, http://www.clontech.com/). For 5′-RACE and 3′-RACE analysis, a specific antisense primer (F78GSP1) and a specific sense primer (F78GSP2) were used (Table S1), respectively.

To recover the internal sequence of the transcripts, RT-PCR was performed by using DNase I and SuperScript II (Invitrogen) according to the manufacturer's instructions. Primers (F78RT1 to F78RT4) were designed according to the sequences within the boundaries defined by the exon ends (Table S1) for PCR amplification of the reverse-transcription products. All the PCR products were ligated

to the pGEM-T vector (Promega, http://www.promega.com/) and sequenced using T7 and SP6 primers.

Generating PAIR3 RNAi transgenic plants

A 392-bp fragment in the second exon of *PAIR3* was amplified by PCR using F78DiF and F78DiR primers (Table S1). The PCR product was cloned to the vector pDS1301 (Yuan *et al.*, 2007) in an inverted repeat orientation. The RNAi construct was introduced into *A. tumefaciens* EHA105 and then into the *japonica* cultivar Zhonghua 11 by *Agrobacterium*-mediated transformation as previously described (Wu *et al.*, 2003).

Histological analyses

Observation of flower development was performed on standard paraffin and plastic sections as described by Hong *et al.* (1995). Panicles of various flower development stages (0.5–24 cm) were fixed in a solution containing 50% ethanol, 5% acetic glacial and 3.7% formaldehyde for 24 h at room temperature, replaced with 70% ethanol twice and stored in 70% ethanol at 4°C until use. For observation of anther development, the anthers at different developmental stages were dehydrated through an ethanol series, embedded into Technovit 8100 resin (Heraeus Kulzer, http://www.heraeus-kulzer.com/) and polymerized at 37°C for 3 days. The samples were sectioned into 1-μm thick slices with a Leica microtome (http://www.leica.com/), mounted on slides and stained with 0.25% toludine blue O (Merck, http://www.merck.com). For the observation of embryo sac development, the ovaries at different developmental stages were stained with Ehrlich's hematoxylin for 3 days, replaced with distilled water three times at intervals of 3 h each time, rinsed in tap water several times at intervals of 2 h each time until the samples became blue, and then dehydrated through an ethanol series, substituted with xylene and embedded into paraffin. The samples were sectioned to a thickness of 8 μm with a rotary microtome. All the slides were photographed with a Leica DM4000 B microscope. Images were enhanced with Photoshop CS.

Pollen meiotic chromosome observation

The young panicles (4.0–6.0 cm in length) at meiosis stage were fixed with 5:3:2 of 95% ethanol:glacial acetic acid:chloroform for 24 h at room temperature, replaced with 70% ethanol twice and stored in 70% ethanol at 4°C until observation. The stamens were dissected gently and crushed with a needle, mounted on a glass slide with a drop of improved karbol fuchsin and photographed using a Leica DM4000 B microscope. Images were enhanced with Photoshop CS.

RT-PCR analyses

Total RNA was isolated from roots, stem, leaf sheath, leaves and young panicles from the WT and *pair3* mutants. Two micrograms of total RNA was reverse transcribed by M-MLV RT (Promega) with the oligo$(dT)_{20}$ primer. The RT-PCR was performed in an ABI 9700 thermocycler (Applied Biosystems, http://www.appliedbiosystems.com/) with the following cycling profile: 94°C for 5 min; 23–38 cycles at 94°C for 45 sec, 55°C for 45 sec and 72°C for 1.5 min; and 72°C for 10 min. The expression pattern of *PAIR3*, *PAIR1*, *PAIR2*, *MEL1*, *OsDMC1*, *OsRAD21-4* and the standard control *Actin* gene were examined by RT-PCR with specific primers listed in Table S2.

In situ hybridization

Flowers from different developmental stages were fixed in a solution containing 50% ethanol, 5% acetic glacial and 3.7% formaldehyde for 24 h at room temperature, replaced with 70% ethanol twice and stored in 70% ethanol at 4°C. They were dehydrated through an ethanol series, substituted with xylene, embedded into paraffin and sectioned to 8 μm. A *PAIR3* cDNA fragment was amplified by PCR with the primer pair F78RT1 (Table S1) and ligated to the pGEM-T vector (Promega). The probe was then transcribed *in vitro* under a T7 or SP6 promoter with polymerase using a digoxigenin (DIG) RNA labeling kit (Roche, http://www.roche.com/). The RNA hybridization and immunological detection of the hybridized probes were performed according to the protocol of Kouchi and Hata (1993).

ACKNOWLEDGEMENTS

We thank Drs Chunli Chen and Jialing Yao for technical assistance. We thank Dr Meizhong Luo for providing the Zhonghua 11 BAC clone a0023B04. We also thank Drs John Bennett and Peter Shaw for helpful comments on the manuscript. This research was supported by grants from the National Special Key Project of China on Functional Genomics of Major Plants and Animals, the National Natural Science Foundation of China and the National Program on Key Basic Research Project (2007CB108700).

SUPPORTING INFORMATION

Additional Supporting Information may be found in the online version of this article:

Figure S1. Phenotype and genotype analysis of the *pair3-2* mutant.

Figure S2. Male meiocyte meiosis analysis of the wild type and the *pair3-2* mutant.

Figure S3. Repressed expression of *PAIR3* in the *pair3-2* mutant.

Table S1. List of the primers used for analyses of the *PAIR3* gene.

Table S2. List of the primers used for semi-quantitative RT-PCR analysis.

Please note: Wiley-Blackwell are not responsible for the content or functionality of any supporting materials supplied by the authors. Any queries (other than missing material) should be directed to the corresponding author for the article.

REFERENCES

Armstrong, S.J., Caryl, A.P., Jones, G.H. and Franklin, F.C.H. (2002) Asy1, a protein required for meiotic chromosome synapsis, localizes to axis-associated chromatin in *Arabidopsis* and *Brassica*. *J. Cell Sci.* **115**, 3645–3655.

Bai, X., Peirson, B.N., Dong, F., Xue, C. and Makaroff, C.A. (1999) Isolation and characterization of *SYN1*, a *RAD21*-like gene essential for meiosis in *Arabidopsis*. *Plant Cell*, **11**, 417–430.

Bass, H.W., Marshall, W.F., Sedat, J.W., Agard, D.A. and Cande, W.Z. (1997) Telomeres cluster de novo before the initiation of synapsis: a three-dimensional spatial analysis of telomere positions before and during meiotic prophase. *J. Cell Biol.* **137**, 5–18.

Bergerat, A., de Massy, B., Gadelle, D., Varoutas, P.C., Nicolas, A. and Forterre, P. (1997) An atypical topoisomerase II from Archaea with implications for meiotic recombination. *Nature*, **386**, 414–417.

Bhatt, A.M., Lister, C., Page, T., Fransz, P., Findlay, K., Jones, G.H., Dickinson, H.G. and Dean, C. (1999) The *DIF1* gene of *Arabidopsis* is required for meiotic chromosome segregation and belongs to the *REC8/RAD21* cohesin gene family. *Plant J.* **19**, 463–472.

Cai, X., Dong, F.G., Edelmann, R.E. and Makaroff, C.A. (2003) The *Arabidopsis* SYN1 cohesin protein is required for sister chromatid arm cohesion and homologous chromosome pairing. *J.Cell Sci.* **116**, 2999–3007.

Caryl, A.P., Armstrong, S.J., Jones, G.H. and Franklin, F.C. (2000) A homologue of the yeast *HOP1* gene is inactivated in the *Arabidopsis* meiotic mutant *asy1*. *Chromosoma*, **109**, 62–71.

Combet, C., Blanchet, C., Geourjon, C. and Deleage, G. (2000) NPS@: network protein sequence analysis. *Trends Biochem. Sci.* **25**, 147–150.

Deng, Z.Y. and Wang, T. (2007) *OsDMC1* is required for homologous pairing in *Oryza Sativa*. *Plant Mol. Biol.* **65**, 31–42.

Feng, J.H., Lu, Y.G., Liu, X.D. and Xu, X.B. (2001) Pollen development and its stages in rice (*Oryza sativa* L.). *Chinese J. Rice Sci.* **15**, 21–28.

Golubovskaya, I.N., Hamant, O., Timofejeva, L., Wang, C.J., Braun, D., Meeley, R. and Cande, W.Z. (2006) Alleles of afd1 dissect REC8 functions during meitic prophase I. *J. Cell Sci.* **119**, 3306–3315.

Hamant, O., Ma, H. and Cande, W.Z. (2006) Genetics of meiosis prophase I in plants. *Annu. Rev. Plant Biol.* **57**, 267–302.

Higgins, J.D., Sanchez-Moran, E., Armstrong, S.J., Jones, G.H. and Frankin, F.C. (2005) The *Arabidopsis* synaptonemal complex protein ZYP1 is required for chromosome synapsis and normal fidelity of crossover. *Genes Dev.* **19**, 2488–2500.

Hirano, T. (2000) Chromosome cohesion, condensation, and separation. *Annu. Rev. Biochem.* **69**, 115–144.

Hollingsworth, N.M., Goetsch, L. and Byers, B. (1990) The *HOP1* gene encodes a meiosis-specific component of yeast chromosomes. *Cell*, **61**, 73–84.

Hong, S.K., Aoki, T., Kitano, H. *et al.* (1995) Phenotypic diversity of 188 rice embryo mutants. *Dev. Genet.* **16**, 298–310.

Jung, K.H., Han, M.J., Lee, Y.S, Kim, Y.W., Hwang, I., Kim, M.J., Kim, Y.K., Nahm, B.H. and An, G. (2005) Rice *Undeveloped Tapetum1* is a major regulator of early tapetum development. *Plant Cell*, **17**, 2705–2722.

Jung, K.H., Han, M.J., Lee, D.Y. *et al.* (2006) *Wax-deficient anther1* is involved in cuticle and wax production in rice anther walls and is required for pollen development. *Plant Cell*, **18**, 3015–3032.

Keeney, S. (2001) Mechanism and control of meiotic recombination initiation. *Curr. Top. Dev. Biol.*, **52**, 1–53.

Kouchi, H. and Hata, S. (1993) Isolation and characterization of novel nodulin cDNAs representing genes expressed at early stages of soybean nodule development. *Mol. Gen. Genet.* **238**, 106–119.

Li, N., Zhang, D.S., Liu, H.S. *et al.* (2006) The rice *Tapetum Degeneration Retardation* gene is required for tapetum degradation and anther development. *Plant Cell*, **18**, 2999–3014.

Liu, J. and Rost, B. (2001) Comparing function and structure between entire proteomes. *Protein Sci.* **10**, 1970–1979.

Liu, X.D., Xu, X.B., Lu, Y.G. and Xu, S.X (1997) The process of embryo sac formation and its stages dividing in rice. *Chinese J. Rice Sci.* **11**, 141–150.

Lupas, A. (1996) Coiled coils: new structures and new functions. *Trends Biochem. Sci.* **21**, 375–382.

Ma, H. (2005) Molecular genetic analyses of microsporogenesis and microgametogenesis in flowering plants. *Annu. Rev. Plant Biol.* **56**, 393–434.

Ma, H. (2006) A molecular portrait of Arabidopsis meiosis. *The Arabidopsis book*, **53**(1), 1–39.

Martinez-Perez, E., Shaw, P. and Moore, G. (2001) The Ph1 locus is needed to ensure specific somatic and meiotic centromere association. *Nature*, **411**, 204–207.

Mercier, R. and Grelon, M. (2008) Meiosis in plants: ten years of gene discovery. *Cytogenet Genome Res.* **120**, 281–290.

Mercier, R., Vezon, D., Bullier, E., Motamayor, J.C., Sellier, A., Lefevre, F., Pelletier, G. and Horlow, C. (2001) SWITCH1 (SWI1): a novel protein required for the establishment of sister chromatid cohesion and for bivalent formation at meiosis. *Genes Dev.* **15**, 1859–1871.

Nonomura, K. I., Nakano, M., Fukuda, T., Eiguchi, M., Miyao, A., Hirochika, H. and Kurata, N. (2004a) The novel gene *HOMOLOGOUS PAIRING ABERRATION IN RICE MEIOSIS1* of rice encodes a putative coiled-coil protein required for homologous chromosome pairing in meiosis. *Plant Cell*, **16**, 1008–1020.

Nonomura, K.I., Nakano, M., Murata, K., Miyoshi, K., Eiguchi, M., Miyao, A., Hirochika, H. and Kurata, N. (2004b) An insertional mutation of rice *PAIR2* gene, the ortholog of *Arabidopsis ASY1*, resulits in a defect in homologous chromosome pairing during meiosis. *Mol. Genet. Genomics*, **271**, 121–129.

Nonomura, K.I., Nakano, M., Eiguchi, M., Suzuki, T. and Kurata, N. (2006) PAIR2 is essential for homologous chromosome synapsis in rice meiosis I. *J. Cell Sci.* **119**, 217–225.

Nonomura, K.I., Morohoshi, A., Nakono, M., Eiguchi, M., Miyao, A., Hirochika, H. and Kurata, N. (2007) A germ cell-specific gene of the ARGONAUTE family is essential for the progression of the premeiotic mitosis and meiosis during sporogenesis in rice. *Plant Cell*, **19**, 2583–2594.

Rockmill, B. and Roeder, G.S. (1998) Telomere-mediated chromosome pairing during meiosis in budding yeast. *Genes Dev.*, **12**, 2574–2586.

Scherthan, H. (2001) A bouquet makes ends meet. *Nat. Rev. Mol. Cell Biol.*, **2**, 621–627.

Stacey, N.J., Kuromori, T., Azumi, Y., Roberts, G., Breuer, C., Wada, T., Maxwell, A., Roberts, K. and Suqimoto-Shirasu, K. (2006) *Arabidopsis* SPO11-2 functions with SPO11-1 in meiotic recombination. *Plant J.* **48**, 206–216.

Sym, M., Engebrecht, J. and Roeder, G.S. (1993) ZYP1 is a synaptonemal complex protein required for meitic chromosome synapsis. *Cell*, **72**, 365–378.

Tsubouchi, T. and Roeder, G.S. (2005) A synaptonemal complex protein promotes homology-independent centromere coupling. *Science*, **308**, 870–873.

Wu, C.Y., Li, X.J., Yuan, W.Y. *et al.* (2003) Development of enhancer trap lines for functional analysis of the rice genome. *Plant J.* **35**, 418–427.

Yuan, B., Shen, X.L., Li, X.H., Xu, C.G. and Wang, S.P. (2007) Mitogen-activated protein kinase OsMPK6 negatively regulates rice disease resistance to bacterial pathogens. *Planta*, **226**, 953–960.

Zhang, J.W., Li, C.S., Wu, C.Y., Xiong, L.Z., Chen, G.X., Zhang, Q.F. and Wang, S.P. (2006a) RMD: a rice mutant database for functional analysis of the rice genome. *Nucleic Acid Res.* **34** (Database issue), D745–D748.

Zhang, L.R., Tao, J.Y., Wang, S.X., Chong, K. and Wang, T. (2006b) The rice OsRad21-4, an orthologue of yeast Rec8 protein, is required for efficient meiosis. *Plant Mol. Biol.* **60**, 533–554.

Zhang, J., Guo, D., Chang, Y.X. *et al.* (2007) Non-random distribution of T-DNA insertions at various levels of the genome hierarchy as revealed by analyzing 13804 T-DNA flanking sequences from an enhancer-trap mutant library. *Plant J.* **47**, 947–959.

Zickler, D. and Kleckner, N. (1999) Meiotic chromosomes: intergrating structure and function. *Annu. Rev. Genet.* **33**, 603–754.

Accession numbers: Sequence data from this article for the cDNA and genomic DNA of *PAIR3* can be found in the GenBank/EMBL data libraries under accession numbers FJ449712 and FJ449711, respectively.

